Article

Optimizing Point Source Tracking in Awake Rat PET Imaging: A Comprehensive Study of Motion Detection and Best Correction Conditions

Fernando Arias-Valcayo [1,*] , Pablo Galve [1,2,3] , Jose Manuel Udías [1,2] , Juan José Vaquero [4,5] , Manuel Desco [4,5,6,7] and Joaquín L. Herraiz [1,2]

1 Grupo de Física Nuclear, Departamento de Estructura de la Materia, Física Térmica y Electrónica & Instituto de Física de Partículas y del Cosmos, Universidad Complutense de Madrid, 28040 Madrid, Spain; pgalve@ucm.es (P.G.); jose@nuc2.fis.ucm.es (J.M.U.); jlopezhe@ucm.es (J.L.H.)
2 Instituto de Investigación Del Hospital Clínico San Carlos (IdISSC), Ciudad Universitaria, 28040 Madrid, Spain
3 Paris Cardiovascular Research Center, Inserm UMR970, Université de Paris, 75015 Paris, France
4 Departamento de Bioingeniería, Universidad Carlos III de Madrid, 28911 Leganés, Spain; jjvaquer@ing.uc3m.es (J.J.V.); desco@hggm.es (M.D.)
5 Instituto de Investigación Sanitaria del Hospital Gregorio Marañón, Unidad de Medicina y Cirugía Experimental, 28009 Madrid, Spain
6 Centro Nacional de Investigaciones Cardiovasculares Carlos III (CNIC), 28029 Madrid, Spain
7 CIBER de Salud Mental Instituto de Salud Carlos III, 28029 Madrid, Spain
* Correspondence: farias02@ucm.es

Abstract: Preclinical PET animal studies require immobilization of the animal, typically accomplished through the administration of anesthesia, which may affect the radiotracer biodistribution. The use of ^{18}F point sources attached to the rat head is one of the most promising methods for motion compensation in awake rat PET studies. However, the presence of radioactive markers may degrade image quality. In this study, we aimed to investigate the most favorable conditions for preclinical PET studies using awake rats with attached point sources. Firstly, we investigate the optimal activity conditions for the markers and rat-injected tracer using Monte Carlo simulations to determine the parameters of maximum detectability without compromising image quality. Additionally, we scrutinize the impact of delayed window correction for random events on marker detectability and overall image quality within these studies. Secondly, we present a method designed to mitigate the influence of rapid rat movements, which resulted in a medium loss of events of around 30%, primarily observed during the initial phase of the data acquisition. We validated our study with PET acquisitions from an awake rat within the acceptable conditions of activity and motion compensation parameters. This acquisition revealed an 8% reduction in resolution compared to a sedated animal, along with a 6% decrease in signal-to-noise ratio (SNR). These outcomes affirm the viability of our method for conducting awake preclinical brain studies.

Keywords: positron emission tomography; awake PET; Monte Carlo; delayed window; random coincidences; anaesthesia; motion correction

1. Introduction

Positron emission tomography (PET) is a powerful tool for imaging biological processes in vivo. PET scans can provide valuable information about molecular mechanisms of disease, drug safety and efficacy, and the response to treatments. In preclinical PET, animal models such as non-human primates and rodents are commonly used to develop and validate novel radiotracers and investigate disease mechanisms. However, the use of anesthesia during preclinical PET scans can have pharmacological effects that may affect physiological parameters, potentially leading to confounding results that limit the translation of preclinical results to the clinic [1–4].

To overcome this limitation, the focus on conducting studies with awake animals has gained importance in recent years. Several approaches have been taken in this field, including the use of restraining devices [5–9], scanners attached to the animals [10,11], and motion tracking and correction techniques. Restraining animals during PET scans can limit the animal's movement but may result in immobilization stress, leading to altered uptake of radiotracers [5,6]. Scanners attached to animals, such as the RatCAP [12,13], offer an alternative approach but may also induce stress in the animal. Motion tracking and correction techniques are currently the most-studied approach, as they allow free animal motion and ensure that the animal is not stressed during the scan.

Within the field of motion tracking and correction, several methods have been proposed. Optical markers [14–17], natural head features [18], point clouds [19], and point sources [20–22] are some of the most widely studied techniques. Optical markers require the rat's head to be facing the tracking camera, and there may be some limitations when the marker is occluded or the bore of the scanner is small. Using natural head features eliminates the need for attaching markers, but to obtain enough distinctive features, it may be necessary to paint a black pattern on the animal's head. Point clouds use a combination of stereo vision and structured light projection to represent the 3D surface of the animal head as point clouds, which can then be used to determine its 3D pose. Finally, point sources attached to the rat head have been widely studied by Miranda et al. [3,20]. This method uses the spatial location of the point sources in the PET data to calculate the head's pose [3]. This approach has shown promising results, making viable the acquisition of awake animal data without requiring any external devices.

Given the potential of using point source markers for motion estimation, our study aimed to optimize the parameters of point source markers strategy, a novel approach in motion tracking and correction. Our primary focus is to evaluate the performance of this motion-correction strategy, both with numerical phantoms as well as with several acquisitions with awake rats, including a reference acquisition of an anesthetized rat for comparison. The purpose of this research is to assess the performance of that method, particularly in situations where motion correction may be challenging. We also investigate when the activity of the point source markers may affect image quality. With these goals in mind, we have conducted a comprehensive analysis to enhance the effectiveness of the point source method and provide valuable insights for its practical applications.

2. Materials and Methods

2.1. Scanner

We have tested our mehtods in a 6R-SuperArgus [23]. The scanner is made up of two layers of 13×13 crystal arrays, each with a crystal pitch of 1.55 mm. The front layer consists of 7 mm-long lutetium–yttrium orthosilicate (LYSO) crystals, while the back layer has cerium-doped 8 mm-long gadolinium orthosilicate (GSO) crystals. The scanner has a total of 6 rings of 24 detectors each, with a radial field of view (FOV) of 17 cm and an axial FOV of 15 cm. Additionally, the scanner acquires data in a single list-mode, with information on the energy, time, and position of each event recorded.

2.2. Point Source Tracking and Motion Compensation

The overall workflow of the reconstruction process is divided into five steps (see Figure 1):
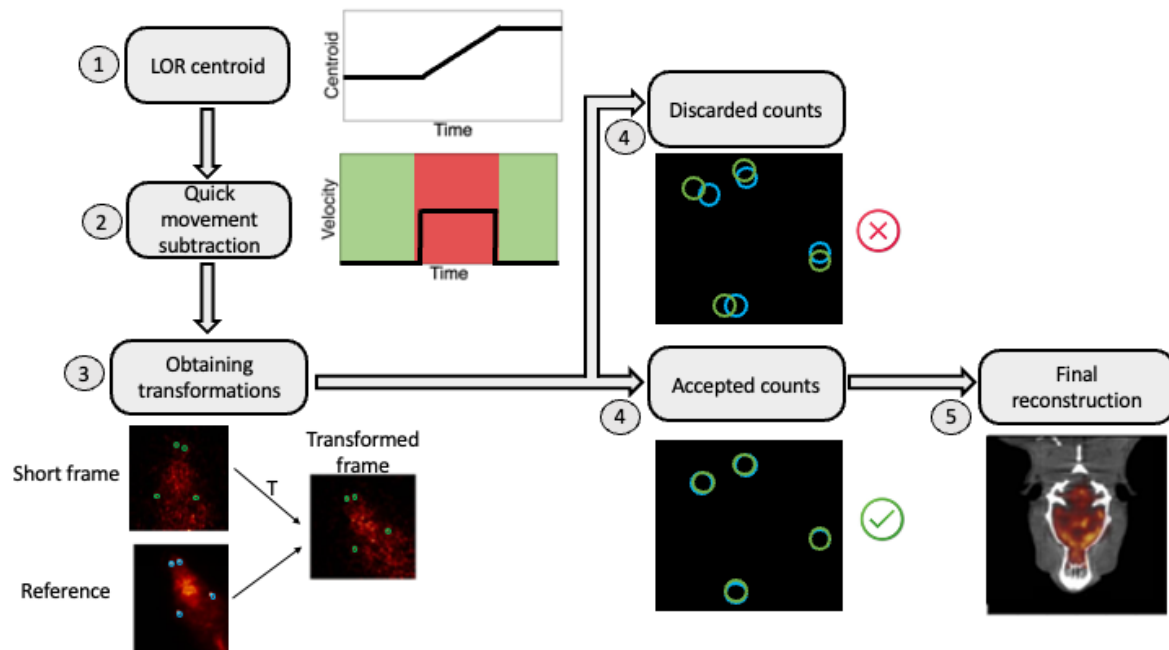
Figure 1. Workflow of the reconstruction process with motion tracking and compensation.

The reconstruction process is divided into five distinct steps, which are described below:

1. **LOR Centroid:** To address motion-related issues, we track the rat's movement during the scan. The centroid position of all LORs is calculated every 50 milliseconds, representing the movement center;

2. **Quick-Movement Subtraction**: Rapid movement is identified using the v_{max} parameter, derived from periods with minimal centroid variation. Such periods are indicative of minimal rat motion. Removing these high-movement intervals helps reduce motion artifacts, vital for small animal studies;

3. **Obtaining transformations**: We use a reference image from the most stable part of the scan. The acquisition is divided into 12.5 ms frames, reconstructed with low iterations while considering rapid movement removal. Rigid transformation matrices are derived by comparing point source locations with the reference;

4. **Non-Precise transformations subtraction**: To assess the quality of our transformations, we calculate a discrepancy measure, χ^2_{fr}, for each frame:

$$\chi^2_{fr} = \frac{\sum_s^N (p_s^{ref} - T(p_s^{fr}))^2}{N} \tag{1}$$

In this equation, N represents the total number of point sources, p_s^{ref} is the position of source s in the reference image, and $T(p^{fr}s)$ is the position of source s in a specific frame fr after applying the transformation T. Frames with χ^2 values below a set limit ($\chi^2 max$) are retained, as rigid transformations may not fully account for the rat's flexible skin, ensuring more accurate image reconstruction;

5. **Final reconstruction**: With the transformation parameters obtained for all frames, we proceed with the reconstruction process. Each event within a frame is transformed based on its corresponding transformation, adjusting scanner positions. As the scanner position changes during reconstruction, we need to adapt the standard Expec-

tation Maximization Maximum Likelihood (EMML) algorithm to ensure accurate reconstruction. We modify sensitivity corrections a_{ij} as follows:

$$a_{ij} = \frac{1}{T_{acq}} \int_0^{T_{acq}} T(t) a_{i'j} dt \tag{2}$$

where T_{acq} is the total acquisition time and $T(t)$ represents the transformation at each time point; it should be noted that voxel i' in $a_{i'j}$ may not correspond to the same voxel i after applying $T(t)$.

2.3. Study of Optimal Conditions for Awake Acquisition with Point Sources

In this study, we aimed to investigate the detectability of point sources in PET imaging using a rat numerical phantom with four point sources and to investigate how these sources affect brain uptake estimation. The phantom was designed with two point sources positioned at the snout and two under the ear.

To evaluate the detectability of point sources and their impact on brain uptake estimation, we explored the effect of different parameters, including the activity of the numerical rat phantom and the activity of the point sources. Specifically, we varied the activity of the rat brain phantom in steps of 20 μCi , ranging from 10 to 210 μCi, and the activity of the point sources in steps of 0.5 μCi, ranging from 1 to 10 μCi. This resulted in a total of 220 combinations of brain and point source activities.

It is important to note that the brain activity simulated in our experiments corresponds to approximately 15% of the total activity in the rat body. This percentage represents the median activity level observed in the brain across the four rat acquisitions explained in Section 2.4. Since the process involves stochastic elements, each combination was simulated 100 times, randomly moving the rat within the FOV to obtain a detectability value for each case.

For each simulation, we used a time step of 12.5 ms (corresponding to a frequency of 80 Hz). This choice of time step strikes a balance between precise motion tracking and good detectability of the sources in the image. The execution time of each simulation was not lengthy due to the short time step. Additionally, to address the introduction of more random coincidences with increasing acquisition activity, we investigated how well the delayed window (DW) method, as proposed by Yavuz et al. [24], can mitigate this issue by subtracting the contribution of random coincidences from the image.

Apart from detectability, we also studied how the activity of the point sources affects image quality. Our primary goal is to study the brain of the animal accurately, which requires avoiding halo artifacts induced by the point sources attached to the animal's head. Halo artifacts are circular regions around high-activity areas, such as the point sources, where nearby regions underestimate the uptake [25]. In addition, we considered the impact of random coincidences introduced by the sources, and we assessed how the DW method can help reduce their impact.

To investigate the effects of point source activity on brain quantification, we conducted simulations with different activities injected into the animal, both with and without point sources. We used the image without point sources as the reference and computed the Root Mean Square Error (RMS_e) for the images with different point source activities. The RMS_e values are defined as

$$RMS_e = \sqrt{\frac{\sum\limits_{j \in BR} (I_j^o - I_j^{ps})^2}{N}} \tag{3}$$

where the sum is performed over the voxels j inside the brain region BR. I^o represents the image without point sources, and I^{ps} represents the image with point sources. N is the total number of voxels inside the brain region. To ensure fair comparison, both images are in relative standardized uptake value (SUV_r).

All simulations took into account scatter and random events to accurately model real-world conditions.

The results of this study enable us to establish the optimal conditions for detecting point sources while avoiding compromising the quality of the reconstructed brain image by adding too much activity.

2.4. Study of Rat Behavior in PET Scanner and How Count Subtraction Affects the Image

The objective of this section is to investigate the effects of rat behavior on PET imaging data, particularly focusing on the impact of subtracting coincidences from the acquisition, as shown in steps 2 and 4 in Figure 1.

To assess the effects of animal behavior on PET imaging data, we conducted a comprehensive study using four different Wistar rats injected with ^{18}F-FDG within the 6R-SuperArgus scanner. During the experiments, the rats were awake. The rats were introduced into a tube that offered freedom of movement. However, the limited diameter of the tube prevented the animals from making full turns, thereby ensuring that they remained within the FOV of the scanner. Acquisitions lasted approximately 600 s for each rat. A primary objective was to identify the parts of the acquisition where the rats moved too quickly, as such movements can adversely affect image quality. Consequently, we subtracted these fastest motion data from the final image reconstruction to improve the overall accuracy.

In one of the rats, four point sources of ^{18}F were placed at the same positions as the simulation shown in Figure 2. This rat is a wistar female rat weighing 255 g. Each point source had an activity of 7 µCi, while the rat's brain had a total activity of 110 µCi at the beginning of the acquisition. Figure 3 shows the rat with the point sources. The study focused on exploring the effects of subtracting more or fewer coincidences by varying the parameters in the reconstruction process. The two parameters that significantly impact the number of counts are v_{max} and χ^2_{max}, as discussed earlier.
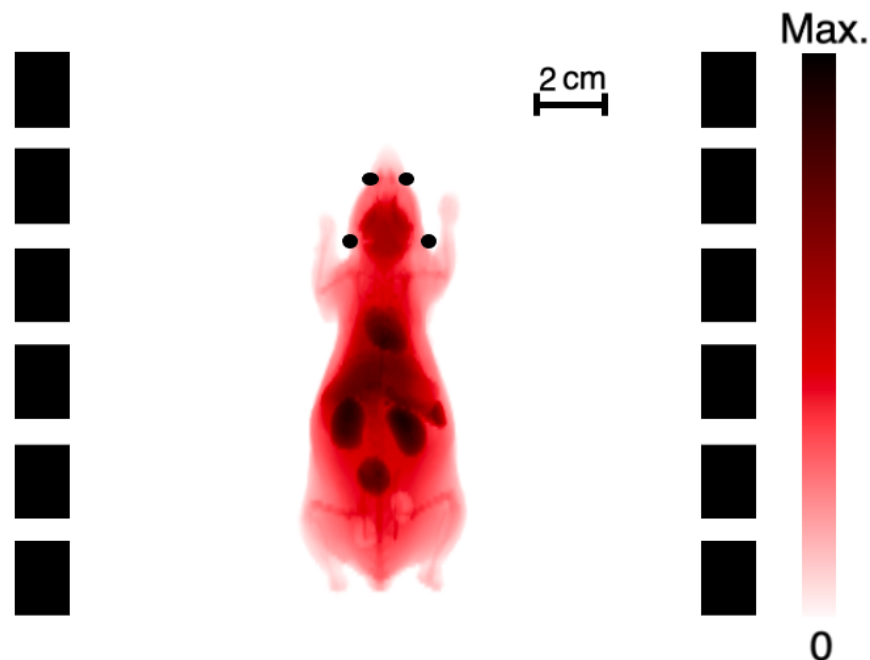

Figure 2. Schematic representation of the numerical rat phantom used in our simulations [26], located inside the 6R-SuperArgus PET scanner. The phantom includes four point sources, two at the snout and two under the ear. The point sources are shown larger than their actual size (1 mm diameter) for visualization purposes.

Figure 3. Rat with the point sources attached to the head.

Two different metrics were used to assess the effect of these parameters and the subtraction of counts. First, we used the point sources attached to the animal's brain to measure the precision of motion compensation by calculating the Full Width at Half Maximum (FWHM) of these sources. The FWHM is a useful measure of spatial resolution that allows us to assess the amount of blurring caused by movement during acquisition.

Secondly, we used the cortex region to measure the signal-to-noise ratio (SNR) , which provides valuable insight into the impact of count subtraction on image quality. SNR is defined by the following formula:

$$\text{SNR} = \frac{\mu}{std} \tag{4}$$

Here, μ represents the mean value inside the region of the cortex, while std denotes the standard deviation within the same region. A higher SNR indicates better image quality with reduced noise.

By analyzing the FWHM and SNR under different conditions, we aim to understand how the movement of rats during PET acquisitions affects image quality and how count subtraction influences the final reconstruction. These insights will contribute to the optimization of point source tracking in Awake Rat PET Imaging, leading to more accurate and reliable data for neuroscience research and other related fields.

2.5. Comparison of Awake vs. Anesthetized Brain Reconstruction

To evaluate the performance of our method, we conducted experiments on a female Wistar rat weighing 255 g, on which four ^{18}F point sources were placed, as detailed in the preceding section. Each point source had an activity of 7 µCi, while the rat's brain had a total activity of 110 µCi at the beginning of the acquisition. The experiments were carried out in two states: under anesthesia and while the rat was awake.

The rat was positioned within the 6R-SuperArgus scanner, initially under anesthesia, with data acquisition commencing just prior to the onset of the awakening process. Each data acquisition session lasted for 600 s. For the anesthetized state, the acquisition yielded a total of 1.55×10^8 coincidences. Once the rat had fully awakened, we performed the second data acquisition, resulting in 1.45×10^8 coincidences.

By comparing the data obtained from the awake and anesthetized states, we gained valuable insights into how motion affected image quality within the context of PET imaging. This comparative analysis enabled us to assess the effectiveness of our motion compensation methods by directly contrasting the resulting images.

3. Results

3.1. Study of Optimal Conditions for Awake Acquisition with Point Sources

The results presented in this section contribute significantly to understanding the relationship between the activity of both the animal and the point sources and the success rate of tracking the point sources. Figure 4 displays the percentage rate of correct tracking of the point sources for frames of 12.5 ms. We have explored how Delayed Window (DW) correction affects detectability, and it is evident that DW correction has a positive impact on the detectability of short frames, expanding the scenarios in which all point sources can be reliably detected. The dash-dotted line serves as a visual representation of the

desired activity configuration in an experiment, where there is a 100% rate of correct tracking of the point sources. This figure demonstrates the effectiveness of the tracking system in high-activity scenarios and provides a reference for optimizing future tracking systems. The results presented in this figure are crucial for guiding experimental design and determining the optimal conditions for point source tracking.
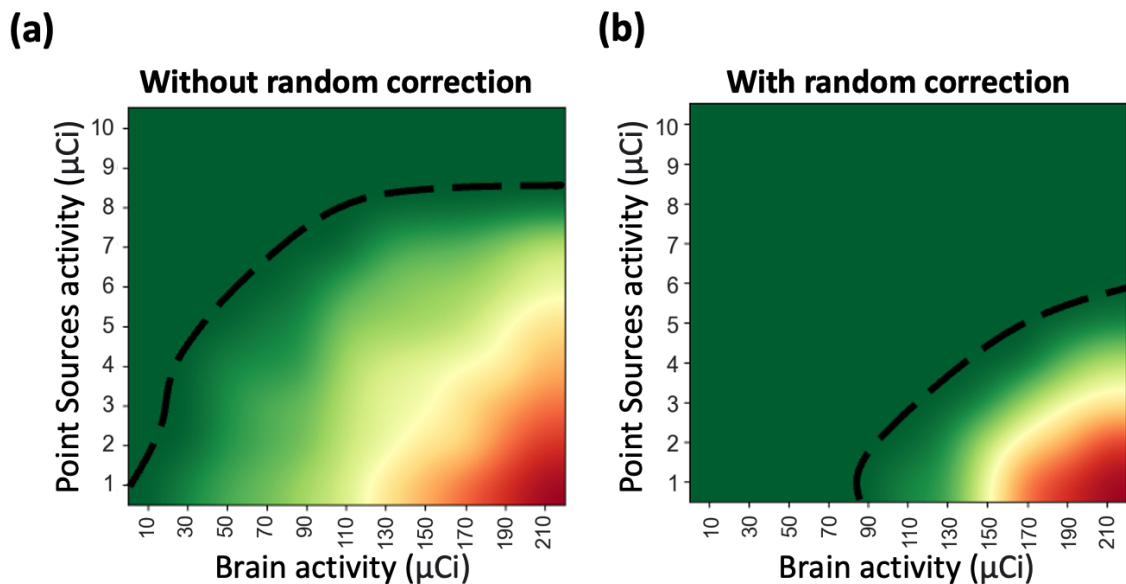
(a)

Without random correction

(b)

With random correction

Figure 4. Point source tracking success as a function of animal and point source activity for frames of 12.5 ms: (**a**) without random correction, (**b**) with random correction using the delayed window method. Since the point source locations are known, the success rate is defined as the percentage of time that all four sources are correctly located. The area above the dashed line represents the ideal activity configuration, where all point sources are tracked with 100% accuracy. This figure is the result of 100 simulations for each configuration.

Next, we investigated how the presence of these point sources affects image quality. Figure 5 illustrates the root mean square error (RMS_e) between the image without point sources and the image with point sources at the injected activity of the animal. All simulations encompassed 450 s of acquisition, considering that our acquisitions are of 600 s, and we estimate a loss of counts of approximately 25% due to the methods of subtraction mentioned in Section 2.2. In this case, DW correction is necessary, as it consistently improves the image quality in all cases. The region below the dash line in Figure 5 represents the range of point source activity that has an RMS_e of less than 0.05, which we consider to have a negligible effect on the quantification of activity in different brain regions of the animal.

By combining the studies on detectability and image quality, we can identify the region of optimal conditions for awake acquisitions with point sources. Figure 6 depicts this region, shown in green. These conditions ensure that the point sources can be tracked every 12.5 ms, and the reconstructed image has a lower degradation than 0.05 RMS_e compared to the image without point sources. The star in the figure represents the conditions of the acquisition analyzed in Sections 3.2 and 3.3.

The information presented in this section provides valuable insights into the best conditions for awake PET imaging with point sources. These findings will contribute significantly to the advancement of motion detection and correction techniques in this field and serve as a foundation for further optimizing tracking systems in future experiments.
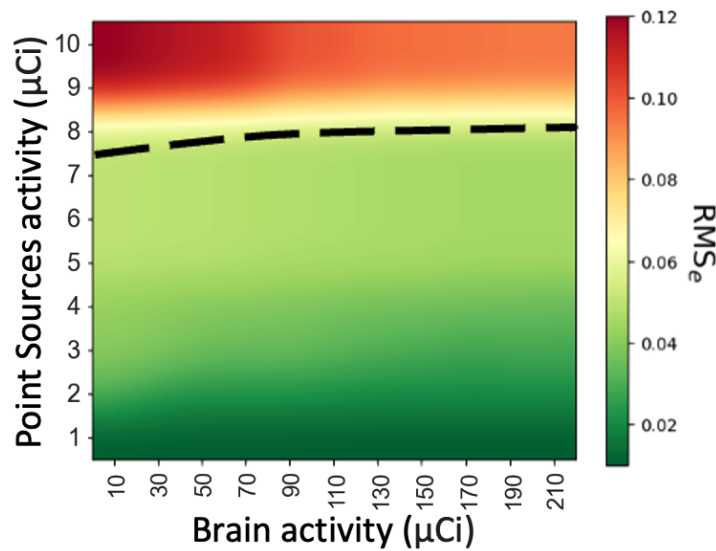
Figure 5. RMS_e as a function of animal and point sources activity for studies with 450 s acquisitions. The region below the dashed line represents the activity configuration that has an RMS_e of less than 0.05. All images have DW correction.
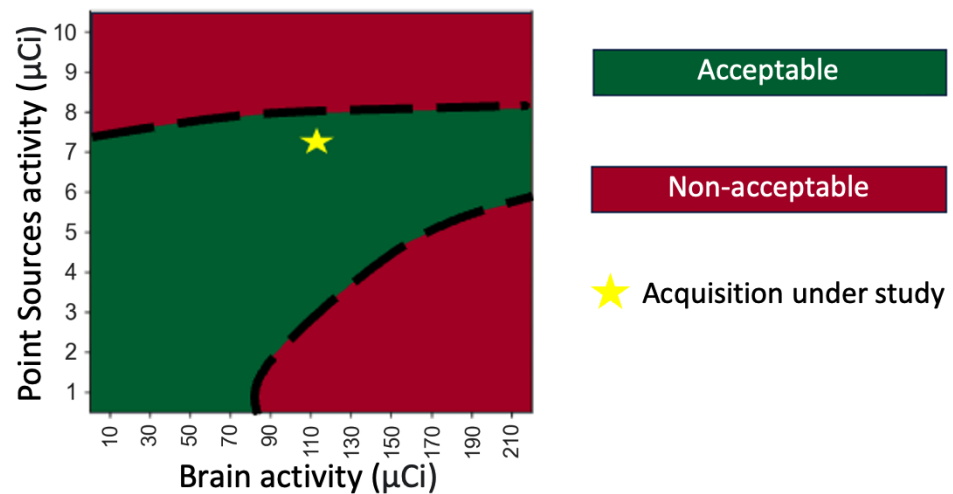

Figure 6. Regions of acceptable and non-acceptable conditions for awake acquisitions as a function of animal and point source activity. The green region represents the area where the sources can be tracked every 12.5 ms, and the image reconstructed has a lower degradation than 0.05 RMS_e with respect to the image without point sources. The star represents the conditions of the acquisition analyzed in Sections 3.2 and 3.3.

3.2. Study of Rat Behaviour in PET Scanner and How Count Subtraction Affects the Image

In this section, our aim is to understand the effect of subtracting counts from the original acquisition. We focus on the subtraction of counts during quick-movement phases. As mentioned before, in order to achieve higher tracking success, we avoid coincidences where the animal is moving quickly, but a trade off between better tracking and count loss is at play. We also investigate the behavior of four different rats inside the 6R-SuperArgus scanner while moving freely in order to identify fast motion periods.

Figure 7 displays the study of the movement of four rats inside the 6R-SuperArgus scanner, showing the centroid of LORs every 50 ms. The areas in green represent regions with low movement, while those in red indicate areas categorized as quick movement. At the top of each graphic, the percentage of events inside low movement frames is shown.

We conducted tests with four different animals to assess the pattern of rat motion inside the scanner and how many events would be removed in our approach. Figure 7

reveals that we retain an average of 73.75% of the counts, with count subtractions ranging from 13.5% in the case with the lowest animal movement to 43.3% in the worst case. We can adjust the v_{max} value to achieve the best reconstruction, as shown shortly.
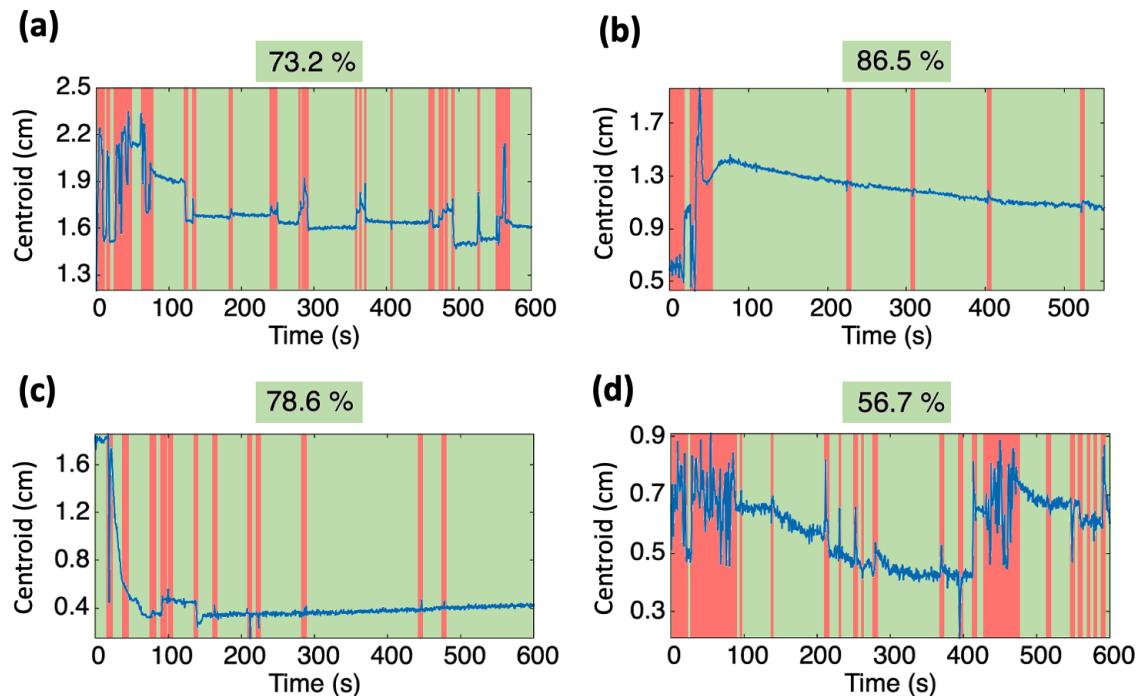

Figure 7. Study of the movement of four rats inside a 6R-SuperArgus scanner. Blue lines show the centroid of LORs every 50 ms. Green areas indicate regions with low movement, while red areas represent regions categorized as quick movement. The percentage of events inside low movement frames is shown at the top of each graphic.

All studies have a total acquisition time of 600 s, providing a sufficient number of events to obtain noise-free images despite possible statistical loss. Additionally, it can be observed that, in most cases, at the early stages of the acquisition, the animal displays significant movement but, after a brief period, relaxes and reduces the amount of movement over time.

Now, we focus on the rat located in the top-left quadrant of Figure 7, which features four point sources attached to its head. The point and rat activities were chosen to lie in the region of optimal conditions, marked with a star in Figure 6. Now, further, we have to adjust two key parameters: v_{max}, which controls the acceptance range for the speed of movement, and χ^2_{max}, which governs the tolerance for accepting less accurate point source position determination. Exploring these parameters enables us to understand the trade off between accepting more or fewer counts.

In Figure 8, we present a comprehensive overview of our study. Panel a shows how higher tolerances in both v_{max} and χ^2_{max} result in keeping more counts in the reconstruction. Panel b shows the trade off between the number of counts used and the apparent size of the reconstructed point sources. This panel suggests that the optimal choice for v_{max} is 1.0 mm/s, as, across different χ^2_{max} values, deviating from this value increases the apparent FWHM of the sources. Additionally, when χ^2_{max} exceeds 0.055, we observe a deterioration in resolution.

Panel c showcases the region of interest (ROI) within the cortex, which is utilized to compute SNR values presented in Panel d. We can see that too strict criteria to accept counts result in pronounced noise in the image, leading to a smaller SNR in the cortex region. Conversely, if we accept nearly all counts, as seen in the right-most case in Figure 9, we introduce noise due to poorly compensated motion, ultimately degrading the

image. The optimal combination of parameters yielding the best SNR and FWHM values is achieved when χ^2_{max} is close to 0.05 and v_{max} is set to 1 mm/s.
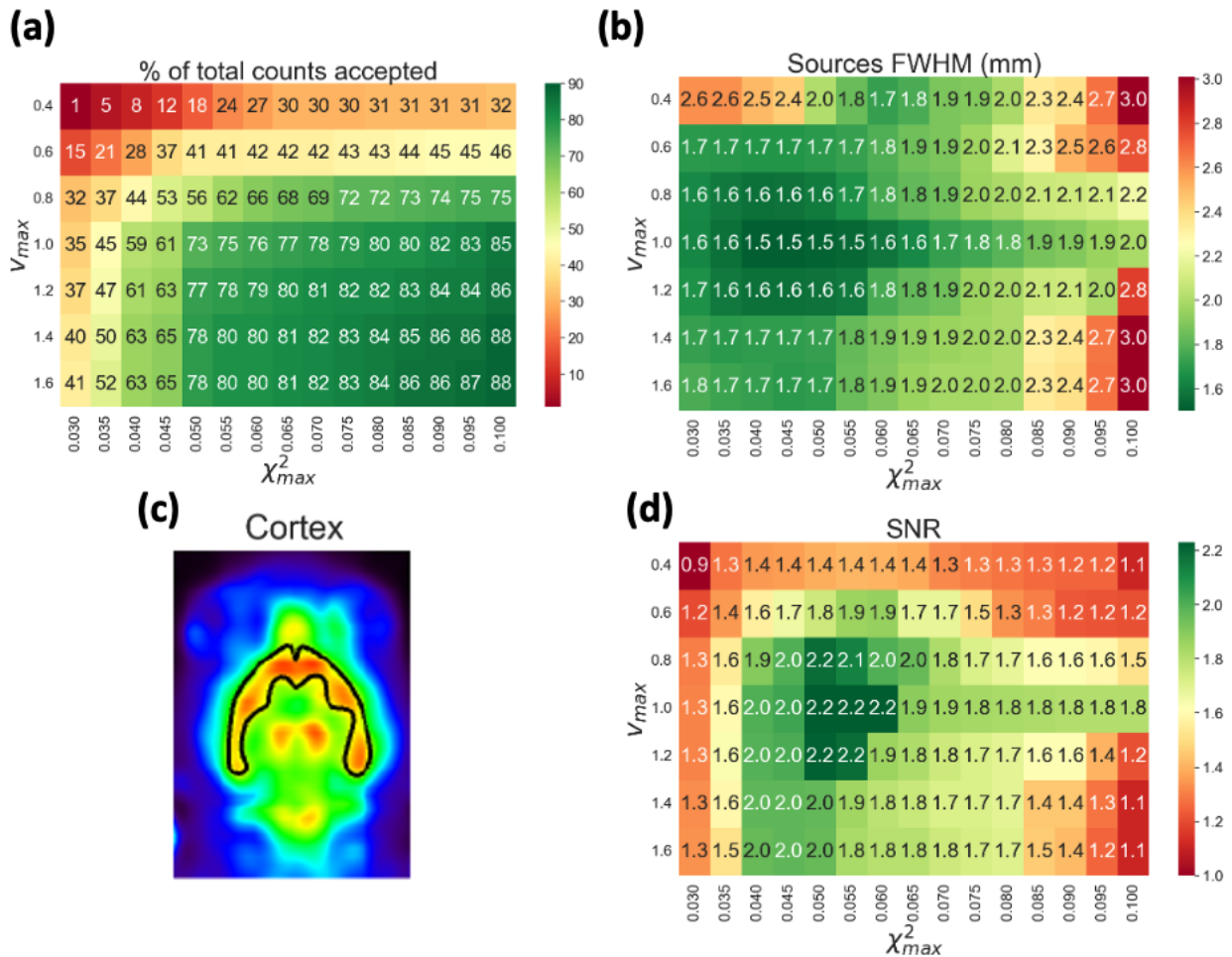

Figure 8. Study on the impact of count subtraction on the image. The total number of coincidences in the acquisitions is 1.45×10^8. (**a**) Percentage of admitted counts for each combination of v_{max} and χ^2_{max}. (**b**) Average FWHM of the four point sources for each case. (**c**) Cortex region utilized for SNR calculation. (**d**) SNR values corresponding to each case.
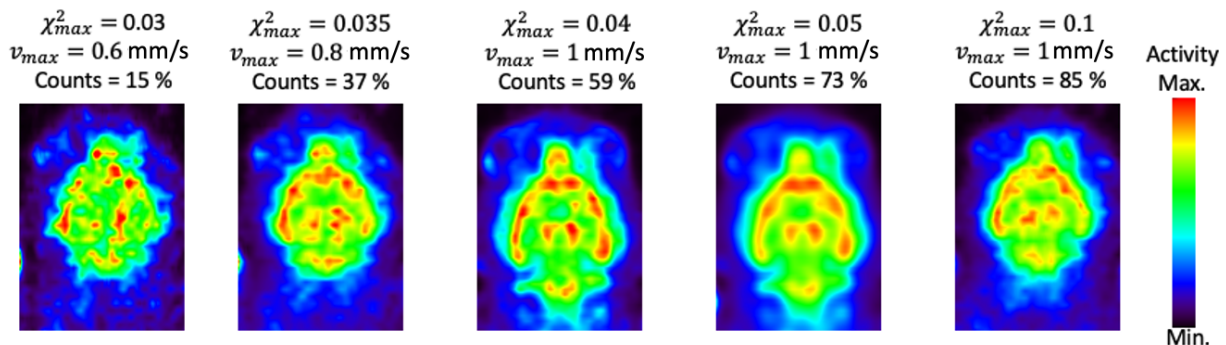
Figure 9. Reconstruction of five different scenarios with varied v_{max} and χ^2_{max}.

3.3. Comparison of Awake vs. Anesthetized Brain Reconstruction

In this section, we compare the imaging results of a rat under anesthesia and in an awake state. The awake state of this acquisition is shown in Figure 7a by its centroid.

In the awake state, 73% of the events were retained after filtering the rapid motion regions, using the best parameters determined in the previous section. Both reconstructions reveal distinguishable brain structures, with only an 8% increase in FWHM of the point sources in the awake rat, with a 6% decrease on SNR at the cortex. Consequently, we can conclude that animal studies can be conducted in awake rats without severely affecting the quantification in brain regions.

4. Discussion

In this study, a primary objective was to optimize the parameters chosen during tracking of point sources in awake rat PET imaging using a motion detection and correction system. We have achieved significant insights that shed light on the factors influencing detectability and image quality in this motion correction strategy.

Initially, we investigated the effects of injected activity on the detectability of point sources attached to the animal. Through extensive simulations, we demonstrated the importance of random correction in ensuring the detection of all point sources. It was also found that that, to obtain image deviations below RMS_e of 0.05 of the reference, requires keeping the activity of the sources below 8 µCi. Additionally, the point sources require a minimum activity when the brain's activity exceeds 90 µCi. While this study was performed using FDG as the tracer, we acknowledge that the activity levels in other organs may vary depending on the tracer used, potentially affecting random coincidences. Therefore, future studies using different tracers should take this into account when optimizing tracking systems.

Next, we addressed the trade off of subtracting coincidences associated with quick-movement and non-precise point source tracking. Through our observations of the four rats within the scanner, as shown in Figure 7, we identified a tendency for these animals to display increased movement during the initial stages of the acquisition. This initial movement could be attributed to the novelty of the environment. However, it became evident that, as the rats acclimated to the scanner, movement reduced.

By optimizing our motion detection and correction parameters, we achieved low noise and excellent image resolution, with the best images obtained when retaining 73% of coincidences for our rat. Remarkably, even with a loss of 27% of coincidences, the impact on image resolution was only 8% and on SNR was 6%, as demonstrated in Figure 10. While our current experiments were conducted with a 10 min acquisition time, future research will explore the potential advantages of longer acquisition durations. Extending the acquisition time may provide an opportunity to capture additional information and enhance imaging sensitivity. However, it is important to recognize that longer acquisition times can introduce challenges related to increased subject movement, necessitating further investigation into the associated motion correction techniques and potential limitations.

We note that the position of the animal's head near the end of the FOV of the scanner may have contributed to the loss of resolution observed. The non-homogeneous resolution across the FOV of the scanner, which exhibits a poorer resolution at the edges of the FOV and could have worsened the image quality. For future studies, it would be beneficial to consider this non-uniform resolution when placing the animal and optimizing motion detection and correction systems for awake rat PET imaging. Additionally, exploring methods to improve the resolution near the edges of the FOV could further enhance image quality in awake rat PET studies [27].

Another important aspect is that, recently, Miranda et al. [28] have proposed adding corrections for cases where point sources shift on the animal's skin. In our approach, instead of trying to correct for these, we remove them from the acquisition by introducing the χ^2 parameter. This way, whether the sources have shifted on the animal or an incorrect transformation has been computed, these counts will not introduce erroneous information into the reconstruction. The loss of counts introduced this way is moderate and can be compensated by a modest increase in acquisition time.
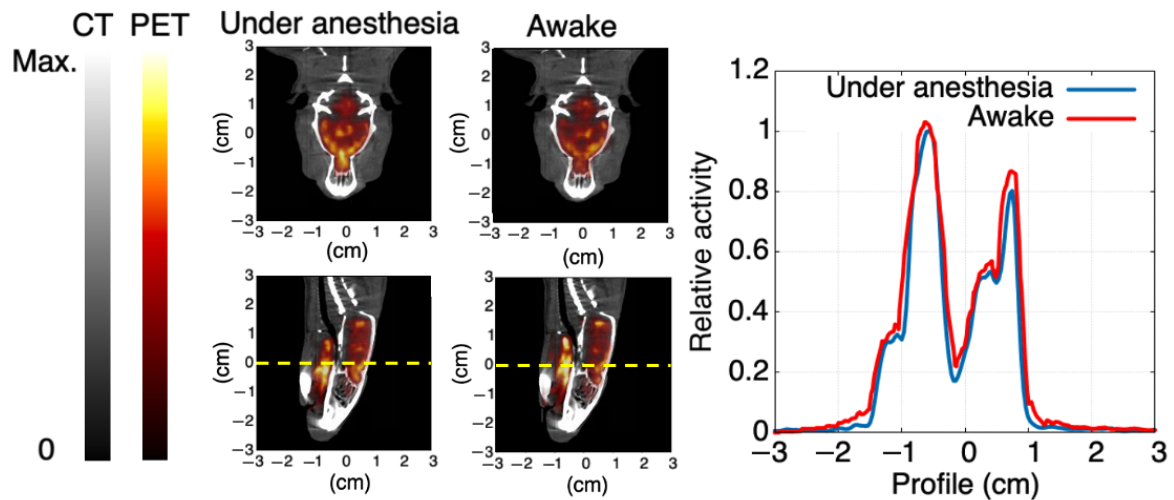
Figure 10. Rat head study with registered CT image in the 6R-SuperArgus scanner. On the **left**, sagittal and coronal views of a rat in both states, awake and under anesthesia. On the **right**, the profile of the yellow dashed line is shown.

5. Conclusions

This study offers valuable insights to optimize the parameters for ^{18}F point source tracking in awake rat PET imaging and establishes a methodology for determining the appropriate marker activity levels relative to rat-injected activity. These levels are scanner-dependent, contingent on sensitivity and resolution. Focusing on the 6R-SuperArgus scanner, we found that random corrections are of great importance and that combining these random correction techniques with carefully selected motion detection and correction parameters ensures comparable image quality to anesthetized acquisitions. By selecting coincidences during periods of no-quick rat motion (approximately 70–80% of acquisition time), we can produce high-quality brain images with only minor resolution reduction, yielding minimal disparities compared to anesthetized rat studies. In summary, we demonstrate that appropriately dosed ^{18}F point markers can facilitate motion detection and compensation in awake rat PET studies, emphasizing the importance of tailoring the approach to study-specific conditions for image comparability with sedated rat studies.

Institutional Review Board Statement: All experimental procedures have been performed in compliance with the European Communities Council Directive 2010/63/EU and submitted for approval by the Institutional Animal Care and Use and Ethics Committee of the Hospital General Universitario Gregorio Marañón (HGUGM), supervised by the Comunidad de Madrid according to the Annex X of the RD 53/2013. The subjects were kept at the animal housing facilities of the Unidad de Medicina y Cirugía Experimental (UMCE-HGUGM) in Madrid, Spain.

Informed Consent Statement: Not applicable.

References

1. Alstrup, A.K.; Landau, A.M.; Holden, J.E.; Jakobsen, S.; Schacht, A.C.; Audrain, H.; Wegener, G.; Hansen, A.K.; Gjedde, A.; Doudet, D.J. Effects of anesthesia and species on the uptake or binding of radioligands in vivo in the Göttingen minipig. *Biomed Res. Int.* **2013**, *2013*, 808713. [CrossRef] [PubMed]
2. Toyama, H.; Ichise, M.; Liow, J.S.; Vines, D.C.; Seneca, N.M.; Modell, K.J.; Seidel, J.; Green, M.V.; Innis, R.B. Evaluation of anesthesia effects on [18F] FDG uptake in mouse brain and heart using small animal PET. *Nucl. Med. Biol.* **2004**, *31*, 251–256. [CrossRef] [PubMed]
3. Miranda, A.; Bertoglio, D.; Stroobants, S.; Staelens, S.; Verhaeghe, J. Translation of preclinical PET imaging findings: Challenges and motion correction to overcome the confounding effect of anesthetics. *Front. Med.* **2021**, *8*, 753977. [CrossRef] [PubMed]
4. Alstrup, A.K.O.; Smith, D.F. Anaesthesia for positron emission tomography scanning of animal brains. *Lab. Anim.* **2013**, *47*, 12–18. [CrossRef] [PubMed]
5. Patel, V.D.; Lee, D.E.; Alexoff, D.L.; Dewey, S.L.; Schiffer, W.K. Imaging dopamine release with positron emission tomography (PET) and 11C-raclopride in freely moving animals. *Neuroimage* **2008**, *41*, 1051–1066. [CrossRef] [PubMed]
6. Sung, K.K.; Jang, D.P.; Lee, S.; Kim, M.; Lee, S.Y.; Kim, Y.B.; Park, C.W.; Cho, Z.H. Neural responses in rat brain during acute immobilization stress: A [F-18] FDG micro PET imaging study. *Neuroimage* **2009**, *44*, 1074–1080. [CrossRef] [PubMed]
7. Hosoi, R.; Matsumura, A.; Mizokawa, S.; Tanaka, M.; Nakamura, F.; Kobayashi, K.; Watanabe, Y.; Inoue, O. MicroPET detection of enhanced 18F-FDG utilization by PKA inhibitor in awake rat brain. *Brain Res.* **2005**, *1039*, 199–202. [CrossRef]
8. Momosaki, S.; Hatano, K.; Kawasumi, Y.; Kato, T.; Hosoi, R.; Kobayashi, K.; Inoue, O.; Ito, K. Rat-PET study without anesthesia: Anesthetics modify the dopamine D1 receptor binding in rat brain. *Synapse* **2004**, *54*, 207–213. [CrossRef]
9. Suzuki, C.; Kosugi, M.; Magata, Y. Conscious rat PET imaging with soft immobilization for quantitation of brain functions: Comprehensive assessment of anesthesia effects on cerebral blood flow and metabolism. *EJNMMI Res.* **2021**, *11*, 46. [CrossRef]
10. Schulz, D.; Southekal, S.; Junnarkar, S.S.; Pratte, J.F.; Purschke, M.L.; Stoll, S.P.; Ravindranath, B.; Maramraju, S.H.; Krishnamoorthy, S.; Henn, F.A.; et al. Simultaneous assessment of rodent behavior and neurochemistry using a miniature positron emission tomograph. *Nat. Methods* **2011**, *8*, 347–352. [CrossRef]
11. Woody, C.; Schlyer, D.; Vaska, P.; Tomasi, D.; Solis-Najera, S.; Rooney, W.; Pratte, J.F.; Junnarkar, S.; Stoll, S.; Master, Z.; et al. Preliminary studies of a simultaneous PET/MRI scanner based on the RatCAP small animal tomograph. *Nucl. Instruments Methods Phys. Res. Sect. Accel. Spectrometers, Detect. Assoc. Equip.* **2007**, *571*, 102–105. [CrossRef]
12. Woody, C.; Kriplani, A.; O'connor, P.; Pratte, J.F.; Radeka, V.; Rescia, S.; Schlyer, D.; Shokouhi, S.; Stoll, S.; Vaska, P.; et al. RatCAP: A small, head-mounted PET tomograph for imaging the brain of an awake RAT. *Nucl. Instruments Methods Phys. Res. Sect. Accel. Spectrometers, Detect. Assoc. Equip.* **2004**, *527*, 166–170. [CrossRef]
13. Vaska, P.; Woody, C.; Schlyer, D.; Pratte, J.F.; Junnarkar, S.; Southekal, S.; Stoll, S.; Schulz, D.; Schiffer, W.; Alexoff, D.; et al. The design and performance of the 2 nd-generation RatCAP awake rat brain PET system. In Proceedings of the 2007 IEEE Nuclear Science Symposium Conference Record, Honolulu, HI, USA, 26 October–3 November 2007; Volume 6, pp. 4181–4184.
14. Kyme, A.Z.; Zhou, V.; Meikle, S.R.; Fulton, R.R. Real-time 3D motion tracking for small animal brain PET. *Phys. Med. Biol.* **2008**, *53*, 2651. [CrossRef] [PubMed]
15. Kyme, A.Z.; Zhou, V.W.; Meikle, S.R.; Baldock, C.; Fulton, R.R. Optimised motion tracking for positron emission tomography studies of brain function in awake rats. *PLoS ONE* **2011**, *6*, e21727. [CrossRef] [PubMed]
16. Spangler-Bickell, M.G.; de Laat, B.; Fulton, R.; Bormans, G.; Nuyts, J. The effect of isoflurane on 18F-FDG uptake in the rat brain: A fully conscious dynamic PET study using motion compensation. *EJNMMI Res.* **2016**, *6*, 1–10. [CrossRef] [PubMed]
17. Miranda, A.; Staelens, S.; Stroobants, S.; Verhaeghe, J. Estimation of and correction for finite motion sampling errors in small animal PET rigid motion correction. *Med. Biol. Eng. Comput.* **2019**, *57*, 505–518. [CrossRef] [PubMed]
18. Torheim, T.; Malinen, E.; Kvaal, K.; Lyng, H.; Indahl, U.G.; Andersen, E.K.; Futsaether, C.M. Classification of dynamic contrast enhanced MR images of cervical cancers using texture analysis and support vector machines. *IEEE Trans. Med. Imaging* **2014**, *33*, 1648–1656. [CrossRef]
19. Miranda, A.; Staelens, S.; Stroobants, S.; Verhaeghe, J. Markerless rat head motion tracking using structured light for brain PET imaging of unrestrained awake small animals. *Phys. Med. Biol.* **2017**, *62*, 1744. [CrossRef]
20. Miranda, A.; Staelens, S.; Stroobants, S.; Verhaeghe, J. Fast and accurate rat head motion tracking with point sources for awake brain PET. *IEEE Trans. Med. Imaging* **2017**, *36*, 1573–1582. [CrossRef]
21. Miranda, A.; Glorie, D.; Bertoglio, D.; Vleugels, J.; De Bruyne, G.; Stroobants, S.; Staelens, S.; Verhaeghe, J. Awake 18F-FDG PET imaging of memantine-induced brain activation and test–retest in freely running mice. *J. Nucl. Med.* **2019**, *60*, 844–850. [CrossRef]

22.   Arias-Valcayo, F.; Herraiz, J.L.; Galve, P.; Vaquero, J.; Desco, M.; Udías, J.M. Awake preclinical brain PET imaging based on point sources. In Proceedings of the 15th International Meeting on Fully Three-Dimensional Image Reconstruction in Radiology and Nuclear Medicine, SPIE, Philadelphia, PA, USA, 2–6 June 2019; Volume 11072, pp. 546–550.

23.   Udias, J.; Gutierrez Fernandez, C.; Herraiz, J.; Perez-Benito, D.; Galve, P.; Lopez-Montes, A.; Lopez-Longas, J.; Arco, J.; Desco, M.; Vaquero, J. Performance evaluation of the PET subsystem of the extended FOV SuperArgus 6R preclinical scanner. In Proceedings of the IEEE Nuclear Science Symposium and Medical Imaging Conference, Sydney, Australia, 10–17 November 2018; pp. 10–11.

24.   Yavuz, M.; Fessler, J.A. Statistical image reconstruction methods for randoms-precorrected PET scans. *Med. Image Anal.* **1998**, *2*, 369–378. [CrossRef]

25.   Heußer, T.; Mann, P.; Rank, C.M.; Schäfer, M.; Dimitrakopoulou-Strauss, A.; Schlemmer, H.P.; Hadaschik, B.A.; Kopka, K.; Bachert, P.; Kachelrieß, M.; et al. Investigation of the halo-artifact in 68Ga-PSMA-11-PET/MRI. *PLoS ONE* **2017**, *12*, e0183329. [CrossRef]

26.   Galve, P.; Arias-Valcayo, F.; Montes, A.; Villa-Abaunza, A.; Ibanez, P.; Herraiz, J.; Udías, J. Ultra-fast Monte Carlo PET Reconstructor. In Proceedings of the 16th International Meeting on Fully 3D Image Reconstruction in Radiology and Nuclear Medicine, Stony Brook, NY, USA, 16–21 July 2021; pp. 152–156.

27.   Arias-Valcayo, F.; Galve, P.; Herraiz, J.L.; Desco, M.; Vaquero, J.J.; Udías, J.M. Reconstruction of multi-animal PET acquisitions with anisotropically variant PSF. *Biomed. Phys. Eng. Express* **2023**, *9*, 065018. [CrossRef]

28.   Miranda, A.; Kroll, T.; Schweda, V.; Staelens, S.; Verhaeghe, J. Correction of motion tracking errors for PET head rigid motion correction. *Phys. Med. Biol.* **2023**, *68*, 175009. [CrossRef]